# LA-UR-24-29648

**Approved for public release; distribution is unlimited.**

**Title:** Verification and Validation of Photonuclear Simulations in LANL Monte Carlo Codes

**Author(s):** Rising, Michael Evan
Bolding, Simon R.
Burke, Timothy Patrick
Giron, Jesse Frank
Haeck, Wim

**Intended for:** Meeting on the International Agreement on Cooperation in Fundamental Science supporting Stockpile Stewardship, 2024-09-18/2024-09-19 (Dijon, France)

**Issued:** 2024-09-16 (rev.1)

Los Alamos
NATIONAL LABORATORY

Los Alamos
NATIONAL LABORATORY

# Verification and Validation of Photonuclear Simulations in LANL Monte Carlo Codes

*Michael E. Rising, *Simon R. Bolding, *Timothy P. Burke,
*Jesse F. Giron, and **Wim Haeck

*Monte Carlo Codes Group, XCP-3, LANL
**Materials and Physical Data Group, XCP-5, LANL

International Agreement on Cooperation in Fundamental Science supporting Stockpile Stewardship
September 18-19, 2024

LA-UR-24-29648

# Outline

Photoatomic and Photonuclear Options in MCNP

Verification with MCATK

Validation with Barber & George Experiments

Other Ongoing Work

MONTE CARLO N-PARTICLE

The MCNP®, Monte Carlo N-Particle®, code can be used for general-purpose transport of many particles including neutrons, photons, electrons, ions, and many other elementary particles, up to 1 TeV/nucleon. The transport of these particles is through a three-dimensional representation of materials defined in a constructive solid geometry, bounded by first-, second-, and fourth-degree user-defined surfaces. In addition, external structured and unstructured meshes can be used to define the problem geometry in a hybrid mode by embedding a mesh within a constructive solid geometry cell, providing an alternate path to defining complex geometry.

Tabulated nuclear and atomic data and/or physics models are used to simulate the physics at each collision a particle undergoes during the transport process. Typically, tabulated nuclear and atomic data are used in the low-energy regime for a subset of projectile particles (e.g., neutrons, photons, light ions) and target nuclei.

Project P213: Verification and Validation of Photonuclear Simulations
CEA Collaborators: Jean-Francois Lemaitre and Amine Nasri
Meetings: Quarterly meetings/exchanges, met in-person 1 March 2024

# Photo- and Electro-atomic Physics in MCNP6

- Photo-atomic Interactions

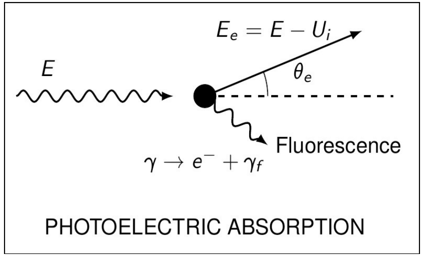


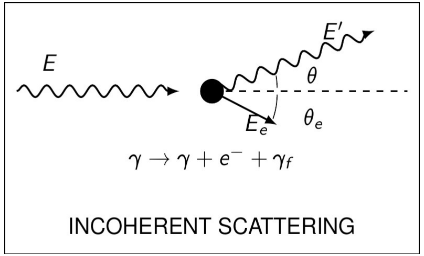


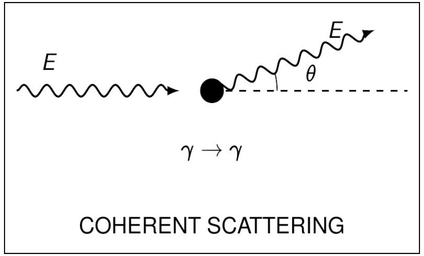


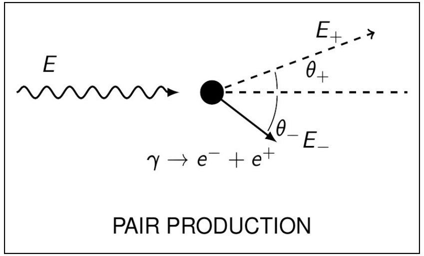


- Electro-atomic Interactions

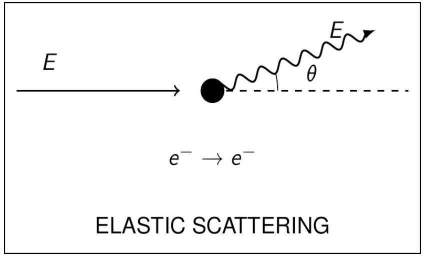


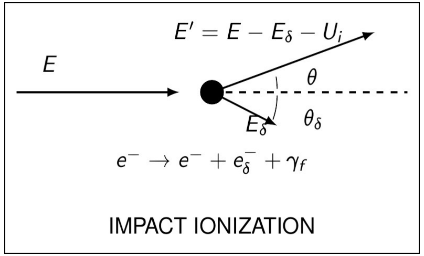


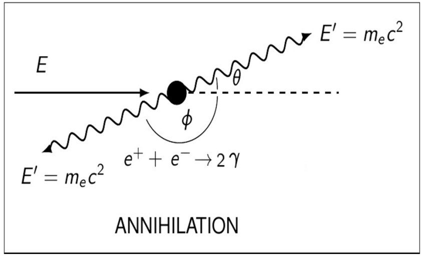


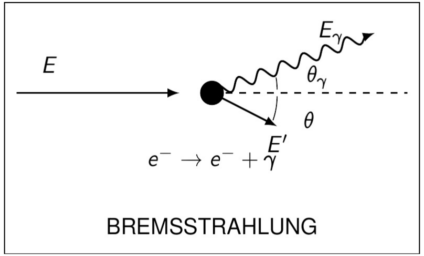


The photon-electron-photon cascade occurs in coupled photon-electron MCNP calculations.

# Motivation for Photonuclear Physics

Uses

- Accelerator neutron source studies – photoneutron production
- Accelerator radiation protection
- Special nuclear materials (SNM) detection and active interrogation concepts
- Medical applications, e.g. therapy

Needs

- More complete tabulated library of photonuclear reaction physics (Latest 2019 IAEA CRP contains 219 nuclides with photonuclear physics data)
  - Compare to 550+ neutron reaction sub-library evaluations in ENDF/B-VIII.0
- Experiment data for photofission evaluation and validation of photonuclear data

# Photonuclear Physics Libraries

- Typical upper energy limit of ~150 MeV
- A photonuclear interaction begins with a photon absorption by a nucleus through the giant dipole resonance or quasi-deuteron absorption
- To be used by MCNP6, libraries are processed into ACE format
- Two libraries have been released with previous versions of the MCNP code

**LA150U**, 13 isotopes, released ~2000

$^{2}$H, $^{12}$C, $^{16}$O, $^{27}$Al, $^{28}$Si, $^{40}$Ca, $^{56}$Fe, $^{63}$Cu, $^{181}$Ta, $^{184}$W, $^{206}$Pb, $^{207}$Pb, $^{208}$Pb

**ENDF7U**, 157 isotopes, released ~2006

- A superset of LA150U, including all 13 isotopes and 144 additional isotopes
- Based on IAEA CRP efforts and ENDF/B-VII.0

- The latest IAEA-2019 CRP makes up the majority of what is in ENDF/B-VIII.1

See Refs. [1-5]

# Photonuclear Physics Models

- Above the ~150 MeV energy threshold physics models can be used directly inline within the MCNP simulation
  - For incident photon energies above the maximum table energy and <1.2 GeV, the cascade-exciton model (CEM) [6] is used by default
  - For incident photon energies >1.2 GeV, the Los Alamos quark-gluon string model (LAQGSM) [7] is used by default

- This kind of inline event generator approach is generally needed in these energy regimes where tabulated data may be difficult to evaluate and validate
  - For photonuclear physics, pion production occurs ~150 MeV where more complex nuclear modeling is needed

$\gamma + {}^{208}Pb$

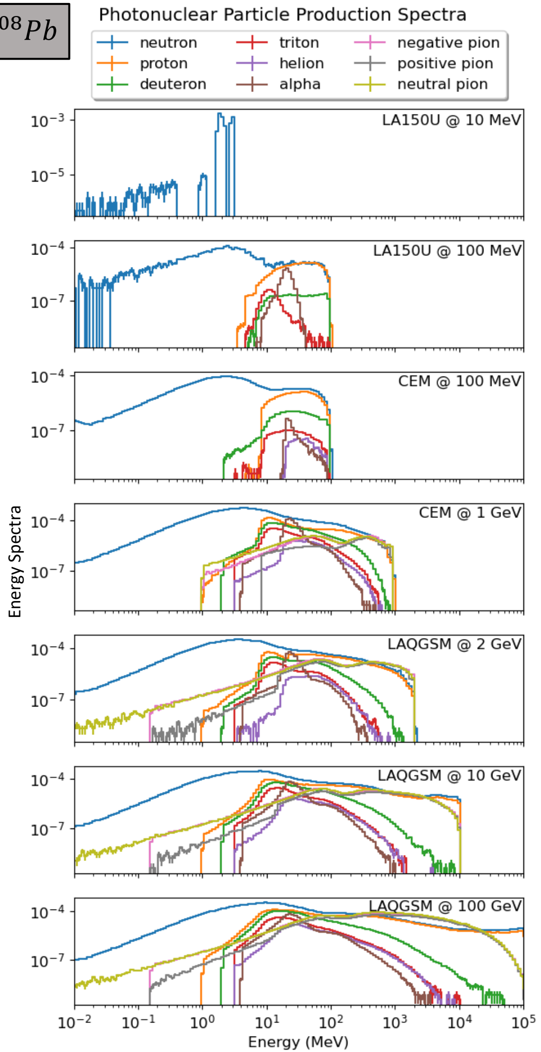

# Other Photonuclear Data and Model Considerations

- In the MCNP code, photonuclear physics is off by default – users must opt-in to make use of this physics

- There is quite a bit of flexibility through a mix-and-match approach within MCNP6 to handle are sorts of physics, including photonuclear interactions
  - Mixed use of model and data above and below an energy threshold
  - Selective use of data and model for any nuclide

- The LLNL Fission Library [8], included in all versions of MCNP6 and in later versions of MCNPX, can be used to simulate photofission reactions for a variety of actinides
  - This library does not use the ACE-based data, but is not quite a physics model event generator like CEM, LAQGSM, etc.

# Photonuclear Physics Enables in MCNP

- Use `ISPN` option on the `PHYS:P` card
  - Both analog and biased photonuclear reaction options available
  - In general, the photonuclear event selection, reaction sampling, and secondary particle production is handled much like all other neutral particles when using the tabulated data

From MCNP6.3.0 User and Theory Manual

**5.7.2.3 Photons (PHYS:P)**

**⚠ Caution**

Former MCNPX users need to be aware that the default behavior of the PHYS:p *nodop* option has changed. Photon Doppler broadening is now on by default (*nodop* = 0).

Data-card Form: PHYS:p *emcpf ides nocoh ispn nodop J fism*

*emcpf* — Upper energy limit for detailed photon physics treatment; photons with energy greater than *emcpf* will be tracked using the simple physics treatment (DEFAULT: *emcpf* = 100 MeV) (1).

*ides* — Controls generation of electrons by photons in MODE p e problems or, in photon-only problems, controls generation of bremsstrahlung photons with the thick-target bremsstrahlung model (2). If

| | |
|---|---|
| *ides* = 0, | then generation is on (DEFAULT). |
| *ides* = 1, | then generation is off. |

*nocoh* — Controls coherent (Thomson) scattering. If

| | |
|---|---|
| *nocoh* = 0, | then coherent scattering is turned on (DEFAULT). |
| *nocoh* = 1, | then coherent scattering is turned off (3). |

*ispn* — Controls photonuclear particle production (4). If

| | |
|---|---|
| *ispn* = −1, | then photonuclear particle production is analog. One photon interaction per collision is sampled. |
| *ispn* = 0, | then photonuclear particle production is turned off (DEFAULT). |
| *ispn* = 1, | then photonuclear particle production is biased. The bias causes a photonuclear event at each photoatomic event. |

*ispn* — Controls photonuclear particle production (4). If

| | |
|---|---|
| *ispn* = −1, | then photonuclear particle production is analog. One photon interaction per collision is sampled. |
| *ispn* = 0, | then photonuclear particle production is turned off (DEFAULT). |
| *ispn* = 1, | then photonuclear particle production is biased. The bias causes a photonuclear event at each photoatomic event. |

# MCATK Photonuclear Verified Against MCNP

**MCATK**

**Abstract.** The Monte Carlo Application Toolkit (MCATK) is a C++ component based Monte Carlo particle transport capability that has been in development by Los Alamos National Laboratory (LANL) since 2008. This paper provides an update on the current capabilities of MCATK, highlighting significant advancements made since the last status report[1]. Notable new features include a Python interface, photon physics, expanded options for geometry modeling, tallies, and source definitions. Additionally, MCATK now offers deterministic weight window generation, stochastic system solution algorithms, shared memory parallelism, and GPU acceleration of ray-tracing tallies. These enhancements have significantly expanded the toolkit's functionality.

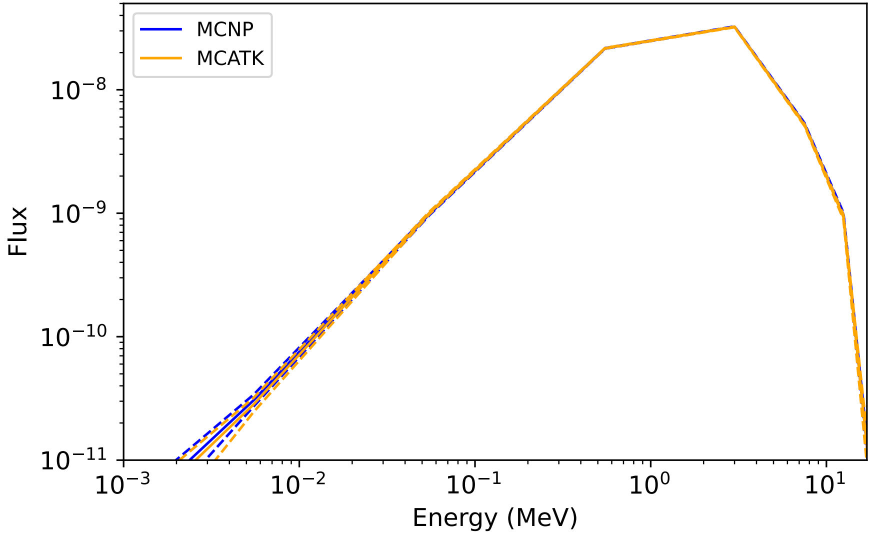


<u>Verification Test</u>

- 1-cm ball of natural U at origin
- Beam of 28 MeV photons
- Next event estimators (point detectors) at (0, 0, 100) and (0, 100, 100)
- Physics turned off in MCNP since MCATK doesn't have it
  - Thick-target bremsstrahlung, Unresolved resonance region, Compton doppler, Photon fluorescence

<u>Summary</u>

- Total neutron flux and spectra agree within 2σ
- Biasing photonuclear interactions in MCNP reduces uncertainty in spectra by ~30% for the same runtime on this simple problem.

# Validation Using Barber & George Experiments

- Electron beam incident on various targets (Al, C, Cu, Pb, Ta, U), measuring the neutron production in the target

PHYSICAL REVIEW VOLUME 116, NUMBER 6 DECEMBER 15, 1959

## Neutron Yields from Targets Bombarded by Electrons*

W. C. BARBER AND W. D. GEORGE†
*High-Energy Physics Laboratory, Stanford University, Stanford, California*
(Received July 21, 1959)

The total neutron yields from thick targets bombarded by electrons were measured as a function of electron energy for the range 10 to 36 Mev. Targets ranging in thickness from one to six radiation lengths of C, Al, Cu, Ta, Pb, and U were used. The yields for 1- and 6-radiation-length targets of Pb at 34 Mev are $2.1\times10^{-3}$ and $9.0\times10^{-3}$ neutrons/electron. Extrapolation to infinite target thickness gives a value of $9.5\times10^{-3}$ neutron/electron. The yield, comparing targets of one radiation length, from C is about 10 times smaller and that from U two times greater than the yield from Pb. An explanation of the relative $Z$-dependence of the yield in terms of known photonuclear cross sections is successful to within a factor of 1.5. The absolute accuracy of the results is estimated to be $\pm15\%$.

Calibration of the neutron-detecting equipment was made with a RaBe source and checked by measuring the yields, due to electro- and photodisintegration of the deuteron, from a heavy-water target. In addition, yields from thin targets of Be and Cu were observed as a function of electron energy. The data for Be yield a value of $(0.018\pm0.003)$ Mev-barn for the $(\gamma,n)$ cross section integrated to 17 Mev. The data for Cu were analyzed and combined with other measurements to give an approximate cross section for the Cu$(\gamma,pn)$ reaction.

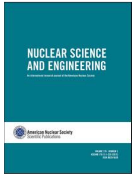


Taylor & Francis

Nuclear Science and Engineering

ISSN: 0029-5639 (Print) 1943-748X (Online) Journal homepage: https://www.tandfonline.com/loi/unse20

## Photonuclear Physics in Radiation Transport—II: Implementation

**M. C. White, R. C. Little, M. B. Chadwick, P. G. Young & R. E. MacFarlane**

**To cite this article:** M. C. White, R. C. Little, M. B. Chadwick, P. G. Young & R. E. MacFarlane (2003) Photonuclear Physics in Radiation Transport—II: Implementation, Nuclear Science and Engineering, 144:2, 174-189, DOI: 10.13182/NSE144-174

**To link to this article:** https://doi.org/10.13182/NSE144-174

- Morgan White (LANL) was responsible for the original photonuclear implementation in MCNP, and modeled the Barber & George experiments for validation purposes

# Barber and George Validation

- Al-I (top) and C-I (bottom) benchmark results shown
- Left panels from M. White using MCNPX
- Right panels using current MCNP6.3 with ENDF7u and ENDF/B-VIII.1beta4 photonuclear data

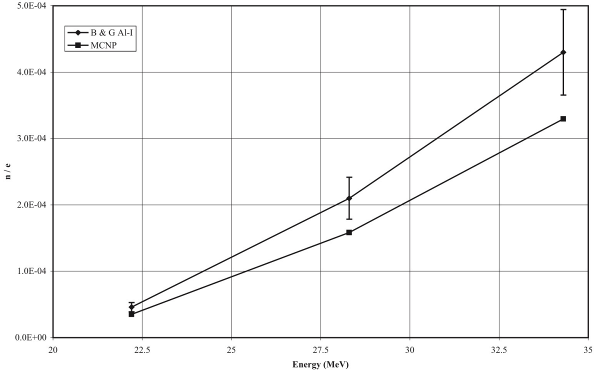


Fig. 1. Neutron yield per electron incident on the Al-I target.

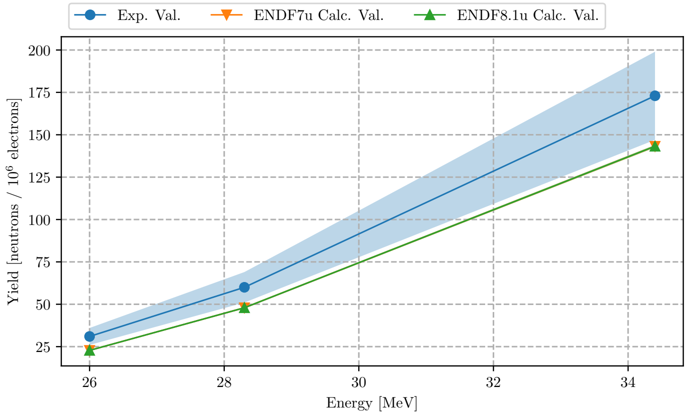


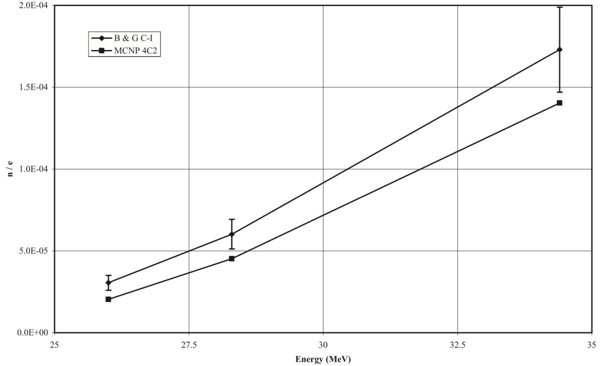


Fig. 2. Neutron yield per electron incident on the C-I target.

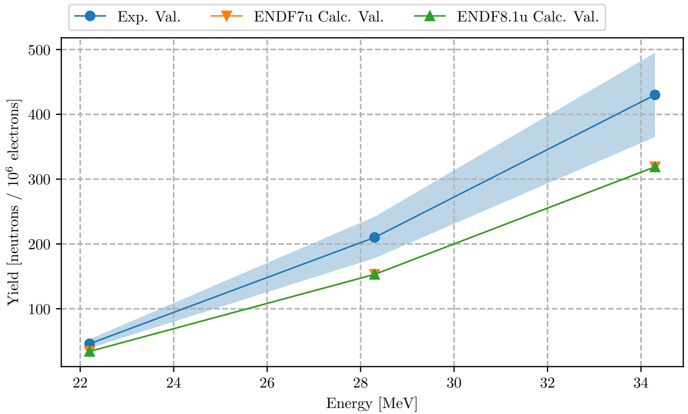

# Barber and George Validation

- Pb-I (top) and C-I (bottom) benchmark results shown
- Left panels from M. White using MCNPX
- Right panels using current MCNP6.3 with ENDF7u and ENDF/B-VIII.1beta4 photonuclear data
  - Problem processing Ta ENDF/B-VIII.1beta4 photonuclear data

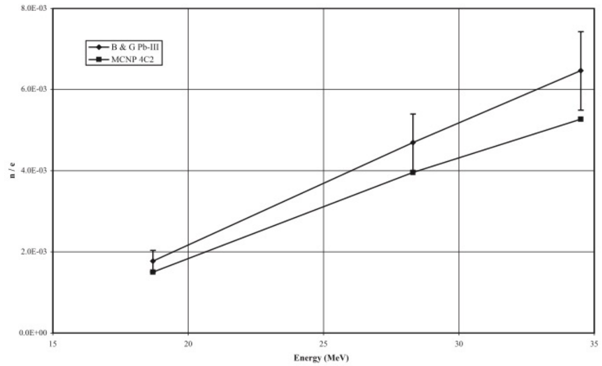

Fig. 10. Neutron yield per electron incident on the Pb-III target.

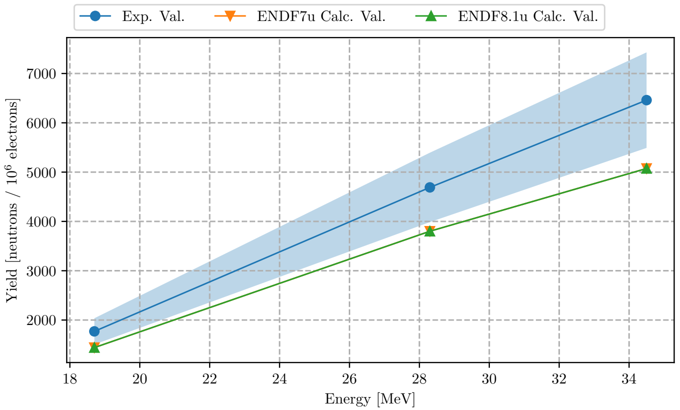


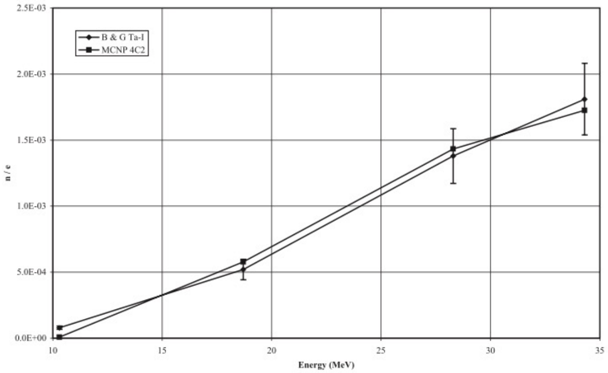

Fig. 13. Neutron yield per electron incident on the Ta-I target.

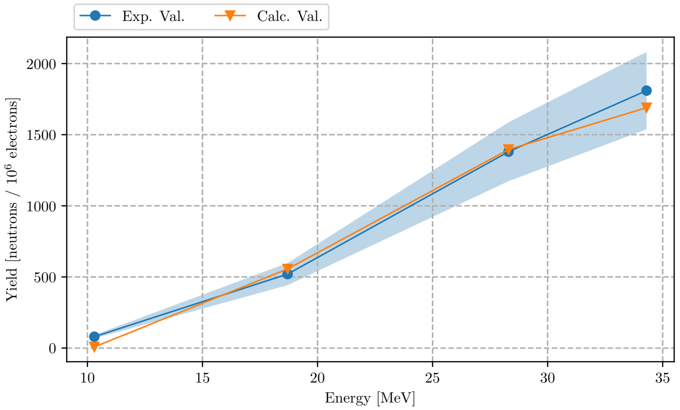

# Barber and George Validation

- Cu benchmarks shown
- Cu-65 photonuclear data appears to be the only change in ENDF/B-VIII.1beta4 that causes differences in these benchmarks
  - This could be because the overall sensitivity to the photonuclear data is limited within the Barber and George benchmarks

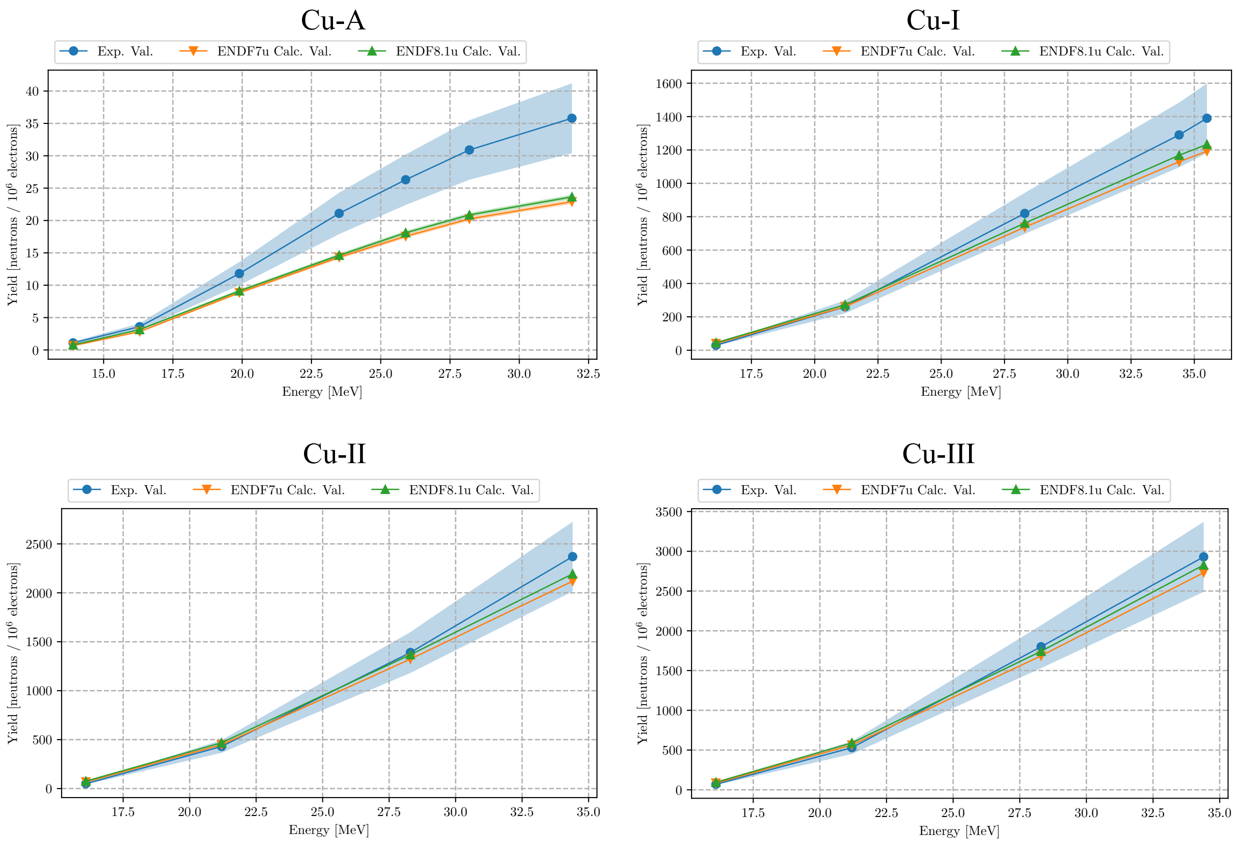

# Ongoing and Future Work

- Process final ENDF/B-VIII.1 photonuclear data files
  - Investigate processing issue with Ta
- More photonuclear verification – pencil beam problems
- Angular-dependent thick-target bremsstrahlung upgrade
  - Not relevant when transporting electrons
  - See backup slide for more information
- Investigate photo- and electro-atomic implementation in MCNP
- Use new CEA photonuclear experiment (SAPHYR) as modern benchmark

# References

[1] P. Oblozinski, ed. "Handbook of Photonuclear Data for Applications." IAEA-TECDOC-1178. International Atomic Energy Association: Vienna, Austria, 2000.

[2] M. B. Chadwick, P. G. Young, R. E. MacFarlane, M. C. White and R. C. Little, “Photonuclear Physics in Radiation Transport: I. Cross Sections and Spectra.” *Nucl. Sci. Eng.*, **144** (2), pages 157–173 (2003). DOI: 10.13182/NSE144-157

[3] M. C. White, R. C. Little, M. B. Chadwick, P. G. Young and R. E. MacFarlane, “Photonuclear Physics in Radiation Transport: II. Implementation.” *Nucl. Sci. Eng.*, **144** (2), pages 157–173 (2003). DOI: 10.13182/NSE144-157

[4] M. B. Chadwick, *et al.*, “ENDF/B-VII.0: Next Generation Evaluated Nuclear Data Library for Nuclear Science and Technology,” *Nucl. Data Sheets*, **107**, 12, 2931 (2006). DOI: 10.1016/j.nds.2006.11.001

[5] T. Kawano, *et al.*, “IAEA Photonuclear Data Library 2019,” *Nucl. Data Sheets*, 163, pages 109–162 (2020). DOI: 10.1016/j.nds.2019.12.002

[6] S. G. Mashnik and A. J. Sierk, “CEM03.03 User Manual,” LANL Report LA-UR-12-01364, Los Alamos, 2012; RSICC Code Package http://www-rsicc.ornl.gov/codes/psr/psr5/psr-532.html; http://www.oecd-nea.org/tools/abstract/detail/psr-0532/.

[7] S. G. Mashnik, K. K. Gudima, N. V. Mokhov, and R. E. Prael, “LAQGSM03.03 Upgrade and Its Validation,” LANL Report LA-UR-07-6198, Los Alamos, 2007; E-print: arXiv:0709.173.

[8] J. M. Verbeke, C. Hagmann, and D. Wright, “Simulation of Neutron and Gamma Ray Emission from Fission and Photofission,” Lawrence Livermore National Laboratory, Livermore, CA, USA, Tech. Rep. UCRL-AR-228518, Jan. 2014.

Thanks!

Questions?

mrising@lanl.gov

# Angular Dependent Thick-Target Bremsstrahlung

- Similar to what is done in the DIANE implementation
  - TTB = Thick-target bremsstrahlung
  - CH = Condensed History
  - ADTTB = Angular-dependent TTB

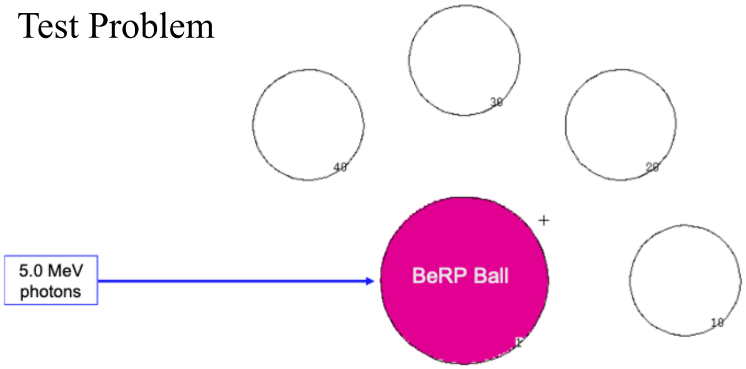


Figure 1: BeRP ball problem setup.

| Angle (deg) | 0 | | 45 | | 90 | | 135 | |
|---|---|---|---|---|---|---|---|---|
| Method | $\phi$ (cm$^{-2}$) | ratio | $\phi$ (cm$^{-2}$) | ratio | $\phi$ (cm$^{-2}$) | ratio | $\phi$ (cm$^{-2}$) | ratio |
| TTB | 1.73e-04 ± 0.21% | 1.43 | 9.32e-06 ± 0.78% | 0.93 | 1.31e-06 ± 2.07% | 0.19 | 1.98e-04 ± 0.17% | 0.67 |
| CH | 1.21e-04 ± 0.24% | 1.00 | 1.00e-05 ± 0.76% | 1.00 | 6.96e-06 ± 0.90% | 1.00 | 2.98e-04 ± 0.14% | 1.00 |
| ADTTB | 1.20e-04 ± 0.24% | 1.00 | 9.73e-06 ± 0.77% | 0.97 | 6.37e-06 ± 0.94% | 0.92 | 3.20e-04 ± 0.13% | 1.07 |
| CH, no $e^{\pm}$ secondaries | 1.21e-04 ± 0.24% | 1.00 | 1.00e-05 ± 0.75% | 1.00 | 6.95e-06 ± 0.90% | 1.00 | 2.98e-04 ± 0.14% | 1.00 |

Table 1: Comparison of flux tallies for BeRP ball problem.

| Angle (deg) | 0 | | 45 | | 90 | | 135 | |
|---|---|---|---|---|---|---|---|---|
| Method | $E\phi$ (MeV cm$^{-2}$) | ratio | $E\phi$ (MeV cm$^{-2}$) | ratio | $E\phi$ (MeV cm$^{-2}$) | ratio | $E\phi$ (MeV cm$^{-2}$) | ratio |
| TTB | 6.00e-04 ± 0.07% | 1.14 | 1.28e-05 ± 0.27% | 0.88 | 1.08e-06 ± 0.70% | 0.11 | 9.18e-05 ± 0.06% | 0.49 |
| CH | 5.25e-04 ± 0.25% | 1.00 | 1.46e-05 ± 0.82% | 1.00 | 9.49e-06 ± 1.00% | 1.00 | 1.86e-04 ± 0.17% | 1.00 |
| ADTTB | 5.27e-04 ± 0.08% | 1.00 | 1.42e-05 ± 0.26% | 0.97 | 8.51e-06 ± 0.33% | 0.90 | 1.88e-04 ± 0.05% | 1.01 |
| CH, no $e^{\pm}$ secondaries | 5.25e-04 ± 0.25% | 1.00 | 1.46e-05 ± 0.81% | 1.00 | 9.51e-06 ± 1.00% | 1.00 | 1.86e-04 ± 0.17% | 1.00 |

Table 2: Comparison of energy-weighted flux tallies for BeRP ball problem.

| Method | $N_{\text{brem}}$ / history | $E_{\text{brem},tot}$ / history |
|---|---|---|
| TTB | 7.85 | 7.6439E-01 |
| CH | 8.49 | 7.6963E-01 |
| ADTTB | 7.69 | 7.2909E-01 |
| CH, no $e^{\pm}$ secondaries | 7.50 | 7.5189E-01 |

| Method | Relative Speedup |
|---|---|
| TTB | 502.6 |
| CH | 1.0 |
| ADTTB | 19.6 |
| CH, no $e^{\pm}$ secondaries | 6.0 |